Proton Uptake upon Anaerobic Reduction of the Paracoccus denitrificans Cytochrome c Oxidase: A Kinetic Investigation of the K354M and D124N Mutants

8 AUTHORS, INCLUDING:

Elena Forte
Sapienza University of Rome
65 PUBLICATIONS **1,339** CITATIONS

SEE PROFILE

Paolo Sarti
Sapienza University of Rome
174 PUBLICATIONS **3,259** CITATIONS

SEE PROFILE

Alessandro Giuffrè
Italian National Research Council
98 PUBLICATIONS **2,361** CITATIONS

SEE PROFILE

Proton Uptake upon Anaerobic Reduction of the *Paracoccus denitrificans* Cytochrome *c* Oxidase: A Kinetic Investigation of the K354M and D124N Mutants[†]

Elena Forte,[#] Francesca Maria Scandurra,[#] Oliver-Matthias H. Richter,[‡] Emilio D'Itri,[#] Paolo Sarti,[#] Maurizio Brunori,[#] Bernd Ludwig,[‡] and Alessandro Giuffrè*,[#]

Department of Biochemical Sciences and CNR Institute of Molecular Biology and Pathology, University of Rome "La Sapienza", I-00185 Rome, Italy, and Institute of Biochemistry, Molecular Genetics, University of Frankfurt, Biozentrum, D-60439 Frankfurt, Germany

ABSTRACT: The kinetics and stoichiometry of the redox-linked protonation of the soluble *Paracoccus denitrificans* cytochrome *c* oxidase were investigated at pH = 7.2−7.5 by multiwavelength stopped-flow spectroscopy, using the pH indicator phenol red. We compared the wild-type enzyme with the K354M and the D124N subunit I mutants, in which the K- and D-proton-conducting pathways are impaired, respectively. Upon anaerobic reduction by Ru-II hexamine, the wild-type enzyme binds 3.3 ± 0.6 H^+/ aa_3, i.e., approximately 1 H^+ in excess over beef heart oxidase under similar conditions and the D124N mutant 3.2 ± 0.5 H^+/aa_3. In contrast, in the K354M mutant, in which the reduction of heme a_3−Cu_B is severely impaired, ~ 0.8 H^+ is promptly bound synchronously with the reduction of heme *a*, followed by a much slower protonation associated with the retarded reduction of the heme a_3−Cu_B site. These results indicate that complete reduction of heme *a* (and Cu_A) is coupled to the uptake of ~ 0.8 H^+, which is independent of both H^+-pathways, whereas the subsequent reduction of the heme a_3−Cu_B site is associated with the uptake of ~ 2.5 H^+ transferred (at least partially) through the K-pathway. On the basis of these results, the possible involvement of the D-pathway in the redox-linked protonation of cytochrome *c* oxidase is discussed.

Cytochrome *c* oxidase (CcOX),[1] the terminal enzyme of the respiratory chain, catalyzes the electron transfer from cytochrome *c* to O_2 to form H_2O. This exergonic reaction is coupled to an active translocation of protons, which generates a proton motive force used for ATP synthesis (*1−3*). The oxygen chemistry takes place at the binuclear heme a_3−Cu_B site, which accepts the electrons donated by the low-spin heme *a*, in turn reduced by cytochrome *c* via the bimetallic Cu_A site. During turnover, the protons involved in the oxygen reduction (chemical protons) and those to be translocated into the P-phase (vectorial protons) come from the N-phase. The uptake and the intramolecular transfer of these protons are intimately connected to the redox chemistry according to a mechanism yet unknown in detail.

The three-dimensional structure of oxidized *Paracoccus denitrificans* CcOX (*4*) allowed the identification of two H^+-conducting pathways, also present in the structure of other heme a_3-containing cytochrome *c* oxidases [from beef heart (*5*), *Rhodobacter sphaeroides* (*6*), and *Thermus thermophilus* (*7*)] as well as in the structure of the bo_3-type quinol oxidase from *Escherichia coli* (*8*). These pathways, denoted as K and D from residues K354[2] and D124 in subunit I, ensure the proton connectivity between the N-phase and the heme a_3−Cu_B binuclear center, which is embedded in the membrane-spanning protein matrix. A third putative proton-conducting pathway, the H-channel, has been suggested first in the bovine enzyme (*5*) and later in the *P. denitrificans* enzyme (*9*); however, site-directed mutagenesis studies on the *Paracoccus* (*10*) and the *Rhodobacter* (*11*) enzymes did not provide support for a functional role of such a pathway.

The K- and D-pathways play different roles in the catalytic cycle, as suggested by transient optical and electrometric measurements on site-directed mutants (see refs *10* and *12* for reviews). The K-pathway should transfer at least one proton during the reductive phase of the catalytic cycle, whereby the heme a_3−Cu_B site is reduced through the sequential transfer of two electrons; according to current models (*13*, *14*), the same pathway could also provide the protons for the subsequent heterolytic cleavage of the O−O

* To whom correspondence should be addressed: Alessandro Giuffrè, Istituto di Biologia e Patologia Molecolari, del Consiglio Nazionale delle Ricerche, c/o Dipartimento di Scienze Biochimiche, Università di Roma "La Sapienza", Piazzale Aldo Moro 5, I-00185 Roma, Italia. Phone: +39-06-4991-0944. Fax: +39-06-4440062. E-mail: alessandro.giuffre@uniroma1.it.

\# University of Rome "La Sapienza".
‡ University of Frankfurt.
[1] Abbreviations: CcOX = cytochrome *c* oxidase; TAME = Nα-*p*-tosyl-L-arginine methyl ester.

[2] Numbering of residues refers to the primary sequence of the *Paracoccus denitrificans* cytochrome *c* oxidase.

bond. All other protons (including those to be pumped) should be transferred through the D-pathway, which begins with residue D124 of subunit I and proceeds up to the residue E278 in the same subunit. From the crystallographic data, it is not clear how the protons are further transferred from E278 to either the heme a_3–Cu$_B$ site (chemical protons) or the exit-pathway up to the P-phase (pumped protons). It was proposed that proton connectivity might be ensured by H$_2$O molecules (*15*, *16*), possibly changing their orientation due to the electric field generated between heme a and the heme a_3–Cu$_B$ site and gating toward the two alternative pathways.

Being a redox-linked proton pump, cytochrome c oxidase must contain ionizable residues whose pK_a depends on the redox/ligation state of the metal centers. These groups, yet unidentified, are at the heart of H$^+$/e$^-$ coupling (*17*, *18*). In view of its significance for the understanding of the proton pumping mechanism, the issue of redox-linked H$^+$ uptake by CcOX has been addressed in a number of studies (*19*–*23*), but several features are still unsettled. To what extent is the D-pathway involved in the proton-transfer coupled to the two-electron reduction of the heme a_3–Cu$_B$ site? It is generally agreed that the proton coupled to the transfer of the *first* electron proceeds through the K-pathway (see for instance refs *2* and *24*); however, the proton associated with the *second* electron transfer is transferred through the D-pathway according to Wikström et al. (*21*), whereas according to Ruitenberg et al. (*25*) it involves the K-pathway, with an additional proton being pumped through the D-pathway. In addition, there is no consensus on the number of protons bound by the enzyme upon reduction of heme a at physiological pH and on the proton-conducting pathways involved (if any). Ruitenberg et al. (*26*) initially proposed that, upon reduction of heme a, one proton is bound through the K-pathway and the process is electrogenic. Later, the Helsinki group (*24*, *27*) assigned this electrogenic proton uptake to the reduction of heme a_3–Cu$_B$ and not of heme a. According to the same group, the reduction of heme a is coupled to a nonelectrogenic, minor H$^+$ uptake (0.2–0.4 H$^+$, as measured on the mixed valence-CO adduct[3] (*21*)), which is independent of both pathways. Finally, the number of protons bound upon anaerobic reduction has been quantitated only for the bovine enzyme (*19*–*23*), but not for a bacterial enzyme or its site-directed mutants.

A kinetic approach to quantitate the redox-linked protonation of beef heart CcOX (*22*) is applied in the present study to the *P. denitrificans* enzyme and mutants of the two proton conducting pathways in subunit I (K354M and D124N). Our data (i) confirm the different roles of the K- and the D-pathways in the reductive phase of the catalytic cycle; (ii) reveal that the total number of protons bound upon complete reduction of the bacterial and the mammalian enzymes is different, and (iii) indicate that the uptake of 0.8 H$^+$ coupled to the reduction of heme a does not involve either one of the two crystallographically determined H$^+$-pathways.

EXPERIMENTAL PROCEDURES

Materials. Dodecyl-β-D-maltoside was purchased from Biomol (Hamburg, Germany); Ru-II hexamine, phenol red,

glucose oxidase, catalase, carbonic anhydrase, trypsin and Nα-p-tosyl-L-arginine methyl ester (TAME) are from Sigma (St. Louis, MO). Experiments were performed at 20 °C and at pH = 7.2–7.5 in the presence of an unbuffered medium containing 50 mM K$_2$SO$_4$ + 0.2% dodecyl-β-D-maltoside. Phenol red (pK_a = 7.8) was used at a concentration of 100 μM. The medium was degassed by N$_2$-equilibration in the presence of 10 μg/mL carbonic anhydrase to reduce the content of carbonated species (see ref *22*); contaminant oxygen was further scavenged by addition of glucose (2 mM), glucose oxidase (8 units/mL), and catalase (260 units/mL).

The wild type and the D124N and K354M subunit I mutants of cytochrome c oxidase (CcOX) were purified from *P. denitrificans* according to ref *28* and kept at −80 °C. Complete oxidation of the K354M mutant was obtained by ferricyanide addition. Prior to use, the enzymes were dialyzed against the aforementioned unbuffered medium, and degassed by N$_2$-equilibration in the presence of 10 μg/mL carbonic anhydrase (see below); immediately before the experiment, glucose, glucose oxidase, and catalase were added. CcOX concentration was determined using the extinction coefficient difference $\Delta\epsilon_{444 \text{ (red−ox)}}$ = 156 mM^{-1} cm^{-1} and is expressed all throughout in terms of functional units (aa_3).

Absorption Spectroscopy. Static spectra were recorded with a double beam spectrophotometer (Jasco V550). Stopped flow experiments were carried out at 20 °C with a thermostated instrument (DX.17MV, Applied Photophysics, Leatherhead, U.K.), equipped with a diode-array. The instrument has a 1-cm light path and can work in a sequential mixing mode, allowing two sequential mixing events with a preset delay time in between. Absorption spectra were collected with an acquisition time of 5 ms according to a logarithmic function of time up to 10 s after mixing. Spectra were collected over the 190–730 nm range (with a resolution of 2.1 nm), but analyzed only in the 470–730 nm range. Data were obtained by averaging three acquisitions and were analyzed by using the software MATLAB (MathWorks, Natick, MA). By using the "left matrix division" algorithm, time-resolved spectra were fitted to a linear combination of reference spectra (heme a, heme a_3 and phenol red) independently collected in the stopped-flow apparatus. The reference redox spectra of heme a and heme a_3 were collected on the wild-type enzyme.

Measurements of Proton Uptake by Cytochrome Oxidase. Measurements of the redox-linked proton uptake by CcOX were performed according to Forte et al. (*22*), by monitoring in the diode-array stopped-flow the anaerobic reduction of oxidized CcOX (~5 μM aa_3) by Ru-II hexamine (30 μM) in the presence of phenol red (100 μM). After correction for a non-redox-linked unspecific signal of the pH dye invariably observed when diluting oxidized CcOX (see ref *22* for details), the optical contributions of phenol red, heme a, and heme a_3 were separated by the "left matrix division" algorithm. The resulting time courses were fitted to the sum of independent exponentials. Calibration of the observed phenol red signals was performed according to Sarti et al. (*29*) making use of TAME, which irreversibly releases 1 H$^+$ per molecule upon hydrolysis catalyzed by trypsin. As specified in ref *22*, proton calibration was performed in the presence of oxidized CcOX (5 μM aa_3) to account for the contribution of the enzyme to the overall buffer power, and

---

[3] The mixed valence-CO derivative is an enzyme with the heme a_3–Cu$_B$ site reduced and CO-complexed, and Cu$_A$ and heme a in the oxidized state.

corrected for the aforementioned unspecific acidification signal. The H^+/enzyme stoichiometries, expressed throughout as 90% confidence intervals, were obtained by dividing the observed redox-linked H^+ concentration changes by the enzyme concentration.

RESULTS

The kinetics and stoichiometry of the redox-linked protonation of the *P. denitrificans* CcOX were investigated by anaerobically mixing the oxidized enzyme with the reductant Ru-II hexamine in the presence of the pH dye phenol red, in unbuffered medium. Upon reduction, the enzyme binds protons from the medium as revealed by an absorption increase of the dye. Ru-II hexamine was chosen because it is a fast, colorless electron donor for CcOX (*30*), and does not release protons on oxidation. To explore the structural basis of the redox-linked protonation, the wild-type enzyme was compared with the D124N and K354M mutants, in which the D- and the K-proton conducting pathways, respectively, are impaired.

Calibration of the Phenol Red Absorption Changes. Following Sarti et al. (*29*), TAME at increasing concentrations was premixed with trypsin and, after a short delay time (30 ms), the resulting mixture was further mixed at pH = 7.2−7.5 with a solution containing oxidized *P. denitrificans* CcOX in the presence of phenol red. In these measurements, the stopped-flow was used in the sequential mixing mode to avoid any possible interaction between TAME and oxidase incubating in the same syringe. Within a few seconds after the second mixing, hydrolysis of TAME releases protons which are revealed by the pH dye. As observed also for the beef heart enzyme (*22*), an unspecific non-redox-linked acidification is invariably observed when diluting oxidized *P. denitrificans* CcOX in the stopped-flow apparatus in the absence of TAME. After correction, acidification is linearly dependent on TAME concentration (Figure 1) and regression analysis yields the difference spectrum of the dye corresponding to a 1 μM change in the bulk proton concentration under the chosen experimental conditions (inset to Figure 1). By comparison with the results previously obtained on the beef heart enzyme under identical conditions (*22*), we note that the buffer power of the bacterial enzyme is ∼20% greater than that of the mammalian enzyme. The buffer power of the D124N and K354M mutants was assumed to be identical to that of the wild-type enzyme.

Redox-Linked H^+ Uptake. In Figure 2 we report the time-resolved absorption changes observed at pH = 7.2−7.5 in the visible region after mixing the oxidized *P. denitrificans* CcOX (wild type, D124N, or K354M) with excess Ru-II hexamine in the presence of phenol red. As already evident from the raw data (Figure 2, left panels), within 10 s the reduction of the enzyme (∼605 nm) and a concomitant bulk alkalinization revealed by deprotonation of phenol red (∼560 nm) are observed. These data were corrected for the unspecific acidification signal seen at the dye band upon enzyme dilution even in the absence of the reductant (Figure 2, inset to left panels); the resulting corrected spectra are reported in the right panels of Figure 2. The unspecific, non-redox-linked acidification was observed with the wild-type enzyme as well as with the two mutants, although it proved to be significantly smaller in the case of the K354M mutant
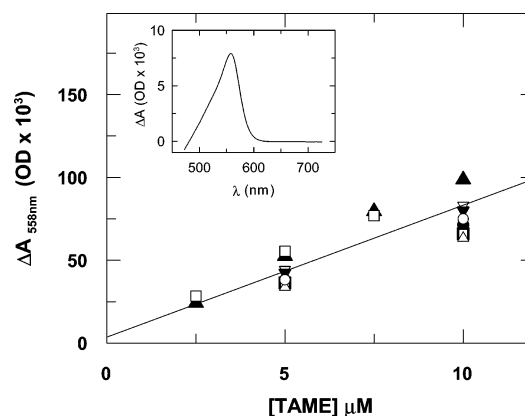

FIGURE 1: Proton calibration. The figure combines the results of eight independent proton calibration experiments (denoted by different symbols), each point being the average of three measurements. Concentrations after mixing were as follows: 0.15 mg mL^{-1} trypsin, 4.0−5.4 μM CcOX (depending on the experiment), and 100 μM phenol red. After correction for the unspecific acidification observed upon CcOX dilution, the observed absorption changes of the dye were linearly dependent on TAME concentration, although a significant variability was observed. The data were pooled and fitted by using the equation $y = \beta x + \alpha_i$, where $i = 1, 2, ..., 8$ was the number of independent calibration experiments performed. From the resulting β value (8.0 ± 0.4 × 10^{-3} OD at 558 nm), we reconstructed the difference spectrum of the dye corresponding to a 1 μM change in the bulk H^+ concentration (inset).

(Figure 2, inset to left panels). Such an acidification, not observed by omitting the enzyme from the reaction mixture, apparently involves a slow (seconds) proton release from the enzyme involving the K-pathway.

From examination of the absorbance changes at ∼560 nm in Figure 2 (right panels), it is evident that within 10 s the apparent redox-linked protonation of the D124N mutant is comparable to that of the wild-type enzyme, whereas over the same time scale it is much smaller for the K354M mutant. The optical contribution of heme *a*, heme *a₃*, and phenol red was separated, and the result of this analysis is reported in Figure 3, showing the time courses of the three optical components. The kinetics of heme *a* reduction is only slightly (if at all) affected by mutations in the two H^+ pathways (Figure 3), the reaction being a little faster in the mutants ($k_1 = 32 ± 6$ s^{-1} and $k_2 = 3.5 ± 1.3$ s^{-1} with relative amplitudes ∼75 and ∼ 25%, respectively) compared to the wild-type enzyme ($k_1 = 23 ± 3$ s^{-1} and $k_2 = 2.3 ± 0.5$ s^{-1} with relative amplitudes ∼70 and ∼30%, respectively). The deviation from a single-exponential behavior of the heme *a* reduction may be due to the limited excess of reductant relative to the enzyme (30 vs 5 μM). Such a deviation may be expected, also considering that electrons equilibrate within the four metal centers in the enzyme at intrinsic rates much faster than the rate of Ru-II hexamine oxidation. The reduction of heme *a₃* is also biphasic both in the wild-type enzyme ($k_1 = 6.7 ± 1.4$ s^{-1} and $k_2 = 0.3 ± 0.16$ s^{-1} with relative amplitudes ∼70 and ∼30%, respectively) and in the D124N mutant ($k_1 = 6.9 ± 0.7$ s^{-1} and $k_2 = 0.3 ± 0.02$ s^{-1} with relative amplitudes ∼60 and ∼40%, respectively), but is totally impaired in the K354M enzyme (Figure 3). It is therefore not surprising that in the K354M mutant, in which electron transfer to heme *a₃*−Cu$_B$ is retarded, the overall H^+ uptake within 10 s is significantly smaller than in the wild-type and the D124N enzymes (Figure 3), which are instead completely reduced over the same time scale.
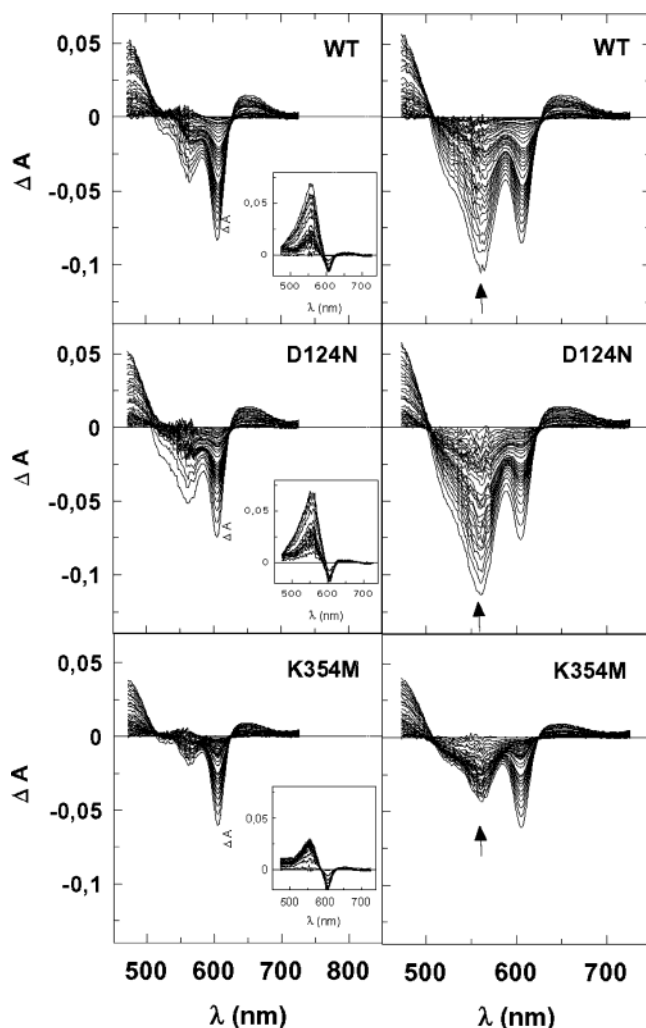
FIGURE 2: Time course of reduction and protonation of the *P. denitrificans* oxidase. The left panels display the absorption spectra collected within 10 s after mixing Ru-II hexamine with oxidized *P. denitrificans* CcOX under anaerobic conditions and in the presence of phenol red. Concentrations after mixing were as follows: 4.4 μM wild-type CcOX (or 5.4 μM D124N mutant or 3.9 μM K354M mutant), 30 μM Ru-II hexamine, and 100 μM phenol red. The results are shown as difference spectra with reference to the endpoint spectrum (acquired at 10 s). The insets display the unspecific acidification observed in the absence of the reductant, which was used to obtain the corrected spectra shown in the right panels. It may be seen that contrary to the D124N mutation the K354M mutation leads to a substantial decrease of the redox-linked protonation of the enzyme occurring within 10 s (see arrows).

The number of protons bound by the enzyme upon reduction (obtained using the calibration of the phenol red absorption changes, Figure 1) and the corresponding time courses are depicted in the bottom panel of Figure 3. Within 10 s, slightly less than 2 H$^+$ are bound upon reduction of the K354M mutant, whereas >3 H$^+$ are taken up in the wild-type enzyme and in the D124N mutant. From several experiments, we estimated the following overall H$^+$/enzyme stoichiometries: 3.3 ± 0.6 H$^+$ ($n = 12$) for the wild-type enzyme; 3.2 ± 0.5 H$^+$ ($n = 8$) for the D124N mutant; and 1.7 ± 0.3 H$^+$ ($n = 6$) for the K354M mutant. Thus, contrary to the K354M mutation, the D124N mutation does not affect significantly the total number of protons bound by CcOX within 10 s.
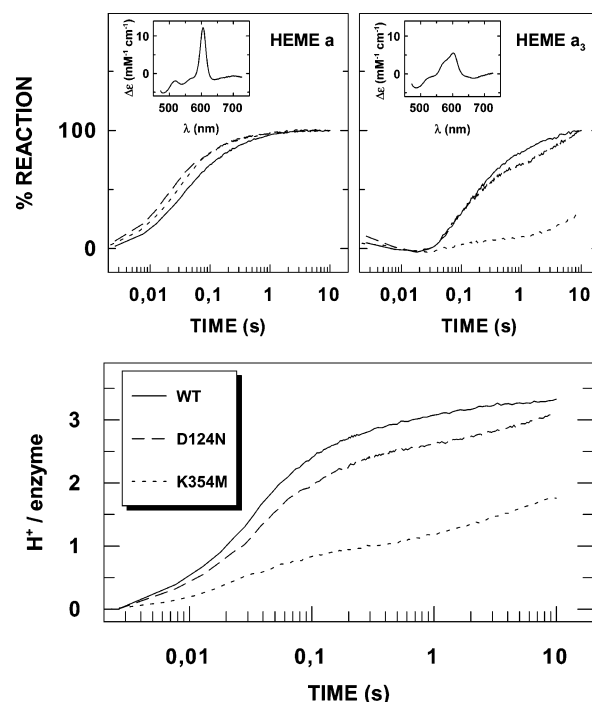

FIGURE 3: Kinetic analysis of the redox-linked protonation. The reduction time courses of heme a and heme a_3 were separated from the time course of phenol red deprotonation by analysis of the spectra in the right panels of Figure 2. Insets: reference redox spectra of heme a (left) and heme a_3 (right). The signal of the pH indicator was calibrated using the information in Figure 1 (inset) and normalized to the enzyme concentration to yield the H$^+$/enzyme stoichiometry. The time course of reduction of heme a is essentially the same in the wild-type enzyme and in the two mutants D124N and K354M, whereas the K354M mutant displays a severely retarded reduction of heme a_3. Consistently, a major effect on the kinetics and stoichiometry of the redox-linked protonation (bottom) is observed within 10 s only with the K354M mutant.

Kinetic analysis shows that ∼2.2 H$^+$ in the wild-type enzyme and ∼1.7 H$^+$ in the D124N mutant are bound essentially synchronously with the reduction of heme a (and presumably Cu$_B$), whereas the additional proton (∼1.1 H$^+$ in the wild-type enzyme and ∼1.5 H$^+$ in the D124N mutant) binds to the enzyme at rates apparently compatible with the reduction of heme a_3. In contrast, in the K354M mutant only 0.8 ± 0.1 H$^+$ ($n = 6$) is bound synchronously with heme a reduction, followed by a much slower protonation (about 0.7−0.9 H$^+$) likely coupled to the retarded and partial reduction of the heme a_3−Cu$_B$ site.

DISCUSSION

The redox-linked protonation of the *P. denitrificans* CcOX was investigated by using a quantitative spectrophotometric protocol recently set up working on the beef heart enzyme (*22*). To assess the role of the crystallographically identified K- and D-proton-conducting pathways (*4*) in the redox-linked protonation, we performed a comparative study on the wild-type enzyme and on the K354M and the D124N subunit I mutants. Since in the K354M mutant the reduction of heme a_3 (and Cu$_B$) is much slower than the reduction of heme a (*27, 31−33*), we were able to estimate the number of protons linked to the reduction of just heme a.

Upon complete reduction at pH = 7.2−7.5, the wild-type *P. denitrificans* oxidase binds ∼3.3 H$^+$, i.e., approximately one proton in excess over the bovine enzyme (∼2.3−2.5 H$^+$,

(*19*, *22−23*)). This novel finding implies that either the two enzymes have different sets of redox-linked ionizable residues or the same residues display different redox-linked ΔpK_a's. The two enzymes are not identical in terms of total ionizable groups, as shown by the finding that at pH = 7.2−7.5 the oxidized bacterial enzyme has a pH buffer power $\sim$20% larger than that of the oxidized bovine enzyme (*22*); this result may or may not be correlated to a larger number of residues able to exchange protons in the bacterial oxidase. On the basis of the structure of the two-subunit bacterial enzyme solved at 2.7 Å resolution (*9*), Kannt et al. (*34*) reported electrostatic calculations, suggesting that complete reduction should be associated with binding of 2.5−2.9 H$^+$, of which 1.8 H$^+$ upon reduction of the heme a_3−Cu$_B$ site and 0.7−1.1 H$^+$ upon reduction of heme *a*. Although the measured and the theoretically predicted overall protonation are somewhat different, at the available resolution of the structure the significance of this difference remains to be assessed.

The finding that the *Paracoccus* enzyme binds one proton in excess over the beef enzyme may appear consistent with the proton pumping mechanism proposed for the mammalian oxidase by Yoshikawa's group (*35*). According to this model based on comparison of the crystallographic structures of the bovine enzyme in the fully oxidized and fully reduced state, D51 undergoes a deprotonation upon enzyme reduction. Since the latter residue is absent in the *Paracoccus* enzyme, this may account for the extra proton bound by the bacterial enzyme upon reduction. However, according to a recent FTIR study (*36*), the D51 structural change would be linked to the reduction of the Cu$_A$/heme *a* moiety. It is therefore relevant to assess whether the additional proton is bound by the bacterial enzyme upon reduction of either heme *a* (and Cu$_A$) or heme a_3−Cu$_B$.

This question cannot be easily answered working with the wild-type enzyme, in which the intrinsic rates of electron equilibration between the redox sites are much faster than electron delivery from Ru-II hexamine to Cu$_A$. In the K354M mutant, however, the reduction of heme a_3 is much slower than that of heme *a* (*27*, *31−33*), which allowed us to establish that 0.8 ± 0.1 H$^+$ is bound upon reduction of Cu$_A$ heme *a* (Figure 3, bottom panel). In this mutant Cu$_B$ reduction should not be so fast (*37*) to partially overlap with the reduction of heme *a*, and thus it should not contribute to the measured $\sim$0.8 H$^+$; this is confirmed by electrometric measurements (*27*) showing that electron equilibration with Cu$_B$ is severely retarded and not observable within a few hundred milliseconds. In summary, 3.3 ± 0.6 H$^+$ are bound upon complete reduction of the wild type enzyme, out of which 0.8 ± 0.1 H$^+$ upon reduction of just Cu$_A$/heme *a* (K354M mutant). By subtraction, we infer that 2.5 ± 0.7 H$^+$ are bound upon the two-electron reduction of the heme a_3−Cu$_B$ site (Figure 4), which yields a H$^+$/e$^-$ ratio of 1.25 ± 0.35. As a tentative interpretation for this result, we propose that part of the excess protonation results from a contribution of "Bohr protons", i.e., protons bound in response to redox-coupled conformational changes. Such a hypothesis may be verified when the 3D structure of the *P. denitrificans* oxidase is available at higher resolution.

The H$^+$/heme *a* stoichiometry of 0.8 agrees with the value (0.7−1.1 H$^+$) predicted by electrostatic calculations based on the structure of the *P. denitrificans* CcOX (*34*). A similar
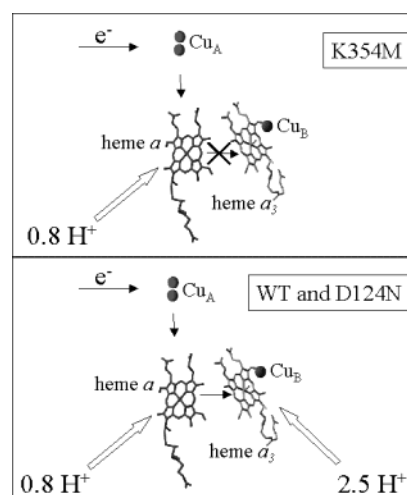

FIGURE 4: Scheme of the redox-linked protonations in oxidase. In the K354M mutant, in which the reduction of heme a_3−Cu$_B$ is severely retarded, $\sim$0.8 H$^+$ is bound synchronously with the reduction of heme *a*, without involvement of either the K- or the D-pathway. By subtraction, we assign the extra $\sim$2.5 H$^+$ bound by the wild-type enzyme and the D124N mutant to the reduction of heme a_3−Cu$_B$.

estimate (0.6−0.7 H$^+$) was obtained with the beef heart enzyme in Triton X-100 (*22*), in which electron transfer to the heme a_3−Cu$_B$ site is much slower and thus kinetically separated from the reduction of heme *a*. Also Capitanio et al. (*20*) reported a similar H$^+$/heme *a* stoichiometry working with the mixed valence-CO bovine enzyme, although a significantly lower value was measured for the same derivative by Verkhovsky et al. (*21*). Given that both in the *Paracoccus* and in the bovine enzyme 0.6−0.8 H$^+$ is coupled to the reduction of heme *a* starting from the fully oxidized species, the extra protonation seen in the bacterial enzyme is linked to the reduction of heme a_3−Cu$_B$ ($\sim$2.5 H$^+$ in the bacterial enzyme and $\sim$1.7 H$^+$ in the bovine enzyme (*22*)). This leads to the conclusion that if the structural change undergone by D51 in the bovine enzyme is linked to the reduction of Cu$_A$/heme *a* (*36*), the absence of D51 in the bacterial enzyme cannot account for the different overall H$^+$ stoichiometry measured in the *Paracoccus* and the bovine oxidases.

The next issue is whether the 3.3 H$^+$ bound upon complete reduction are transferred through the K- and/or the D-pathway. Our results (bottom panel of Figure 3) confirm that at least part of the $\sim$2.5 protons linked to the reduction of the heme a_3−Cu$_B$ site is transferred through the K-pathway (*27*, *31−33*); it remains, however, unclear to what extent the D-pathway is involved. Vygodina et al. (*32*), working on the D124N analogous mutant of the *R. sphaeroides* enzyme, reported a very slight effect of this mutation on the reduction kinetics; hence, the suggestion that the D-pathway *is not* involved in H$^+$ transfer associated to the enzyme reduction. In contrast, according to Wikström et al. (*24*), in the *P. denitrificans* D124N mutant a significant fraction of heme a_3 is reduced at a very low rate (minutes), leading to the suggestion that at least one proton travels through the D-pathway. In our hands, the D124N mutant is fully reduced within 10 s (with no indication of a very slow reduction phase, see also ref *33*) and concomitantly binds essentially the same number of protons as the wild-type enzyme ($\sim$3.2 H$^+$ for the D124N compared to $\sim$3.3 H$^+$). This mutation

only appears to delay the kinetics of binding of $\sim$0.5 H$^+$, as compared to the wild-type enzyme. Anyway, the somewhat marginal effect of the D124N mutation observed in this study has to be reconciled with the greater effects on the reductive phase of the catalytic cycle reported by using different experimental approaches (*25*). As a possible explanation for this discrepancy, we envisage the possibility that a fraction of the 2.5 redox-linked protons are transferred through the D-pathway *quickly* in the wild-type enzyme, but *more slowly* in the mutant; this notwithstanding, the kinetic effect of the mutation on the proton transfer through the D-pathway is minor, and within 10 s this protonation occurs, leaving unchanged the overall stoichiometry, as measured in this study.

A H$^+$/heme *a* stoichiometry of $\sim$0.8, established for the K354M mutant, is not affected by the D124N mutation. As the K354 residue is buried inside the channel (*4*), the surface-exposed subunit II residue E78, recently proposed to be at the entrance of this pathway in the *Rhodobacter sphaeroides* oxidase (*38*, *39*), may be involved. However, mutation E78C does not prevent the fast reduction of heme *a* in the *Rhodobacter* enzyme (*39*). Thus, we conclude that neither the K- nor the D-pathway are involved in the proton uptake associated with the reduction of heme *a*. This is consistent with the finding that the rate of heme *a* reduction is not affected by blocking either pathway (*24*, *32*, *33*), but is in conflict with electrometric measurements on the K354M mutant (*26*), which, although controversial (*27*), suggested an involvement of the K-pathway.

In conclusion, if the proton uptake associated with heme *a* reduction does not involve the K- and/or the D-pathway, the identification of the heme *a* redox-coupled residue(s) remains open. This residue(s) could be on the protein surface or embedded in the membrane-spanning matrix, whereby protonation would affect the extent of electrogenicity of heme *a* reduction by Cu$_A$. Given that, according to proposed mechanisms (*2*, *15*, *17*, *35*, *40*), proton pumping may be coupled to the oxido-reduction of heme *a*, understanding these features is of crucial importance. This issue will be addressed in future studies.

REFERENCES

1. Ferguson-Miller, S., and Babcock, G. T. (1996) Heme/Copper Terminal Oxidases. *Chem. Rev. 96*, 2889−2907.
2. Michel, H. (1999) Cytochrome *c* oxidase: catalytic cycle and mechanisms of proton pumping-A discussion. *Biochemistry 38*, 15129−15140.
3. Zaslavsky, D., and Gennis, R. B. (2000) Proton pumping by cytochrome oxidase: progress, problems and postulates. *Biochim. Biophys. Acta 1458*, 164−179.
4. Iwata, S., Ostermeier, C., Ludwig, B., and Michel, H. (1995) Structure at 2.8 Å resolution of cytochrome *c* oxidase from *Paracoccus denitrificans*. *Nature 376*, 660−669.
5. Tsukihara, T., Aoyama, H., Yamashita, E., Tomizaki, T., Yama-guchi, H., Shinzawa-Itoh, K., Nakashima, R., Yaono, R., and Yoshikawa, S. (1996) The whole structure of the 13-subunit oxidized cytochrome *c* oxidase at 2.8 Å. *Science 272*, 1136−1144.

6. Svennson-Ek, M., Abramson, J., Larsson, G., Törnroth, S., Brzezinski, P., and Iwata, So (2002) The X-ray crystal structures of wild-type and EQ(I-286) mutant cytochrome *c* oxidases from *Rhodobacter sphaeroides*. *J. Mol. Biol. 321*, 329−339.
7. Soulimane, T., Buse, G., Bourenkov, G. P., Bartunik, H. D., Huber, R., and Than, M. E. (2000) Structure and mechanism of the aberrant ba(3)-cytochrome *c* oxidase from *Thermus thermophilus*. *EMBO J. 19*, 1766−1776.
8. Abramson, J., Riistama, S., Larsson, G., Jasaitis, A., Svensson-Ek, M., Laakkonen, L., Puustinen, A., Iwata, So, and Wikström, M. (2000) The structure of the ubiquinol oxidase from *Escherichia coli* and its ubiquinone binding site. *Nat. Struct. Biol. 7*, 910−917.
9. Ostermeier, C., Harrenga, A., Ermler, U., and Michel, H. (1997) Structure at 2.7 Å resolution of the *Paracoccus denitrificans* two-subunit cytochrome *c* oxidase complexed with an antibody F$_V$ fragment. *Proc. Natl. Acad. Sci. U.S.A. 94*, 10547−10553.
10. Pfitzner, U., Odenwald, A., Ostermann, T., Weingard, L., Ludwig, B., and Richter, O. M. (1998) Cytochrome *c* oxidase (heme *aa$_3$*) from *Paracoccus denitrificans*: analysis of mutations in putative proton channels of subunit I. *J. Bioenerg. Biomembr. 30*, 89−97.
11. Lee, H., Das, T. K., Rousseau, D. L., Mills, D., Ferguson-Miller, S., and Gennis, R. B. (2000) Mutations in the putative H-channel in the cytochrome *c* oxidase from *Rhodobacter sphaeroides* show that this channel is not important for proton conduction but reveal modulation of the properties of heme *a*. *Biochemistry 39*, 2989−2996.
12. Brzezinski, P., and Ädelroth, P. (1998) Pathways of proton transfer in cytochrome *c* oxidase. *J. Bioenerg. Biomembr. 30*, 99−107.
13. Konstantinov, A. A. (1998) Cytochrome *c* oxidase as a proton-pumping peroxidase: reaction cycle and electrogenic mechanism. *J. Bioenerg. Biomembr. 30*, 121−130.
14. Pecoraro, C., Gennis, R. B., Vygodina, T. V., and Konstantinov, A. A. (2001) Role of the K-channel in the pH-dependence of the reaction of cytochrome *c* oxidase with hydrogen peroxide. *Biochemistry 40*, 9695−9708.
15. Wikström, M., Verkhovsky, M. I., and Hummer, G. (2003) Water-gated mechanism of proton translocation by cytochrome *c* oxidase. *Biochim. Biophys. Acta 1604*, 61−65.
16. Zheng, X., Medvedev, D. M., Swanson, J., and Stuchebrukhov, A. A. (2003) Computer simulation of water in cytochrome *c* oxidase. *Biochim. Biophys. Acta 1557*, 99−107.
17. Papa, S., and Capitanio, N. (1998) Redox Bohr effects (cooperative coupling) and the role of heme *a* in the proton pump of cytochrome *c* oxidase. *J. Bioenerg. Biomembr. 30*, 109−119.
18. Xavier, A. (2002) A mechano-chemical model for energy trans-duction in cytochrome *c* oxidase: the work of a Maxwell's god. *FEBS Lett. 532*, 261−266.
19. Mitchell, R., and Rich, P. R. (1994) Proton uptake by cytochrome *c* oxidase on reduction and on ligand binding. *Biochim. Biophys. Acta 1186*, 19−26.
20. Capitanio, N., Vygodina, T. V., Capitanio, G., Konstantinov, A. A., Nicholls, P., and Papa, S. (1997) Redox-linked protolytic reactions in soluble cytochrome-*c* oxidase from beef-heart mito-chondria: redox Bohr effects. *Biochim. Biophys. Acta 1318*, 255−265.
21. Verkhosvky, M. I., Belevich, N., Morgan, J. E., and Wikström, M. (1999) Proton linkage of cytochrome *a* oxidoreduction in carbon monoxide-treated cytochrome *c* oxidase. *Biochim. Biophys. Acta 1412*, 184−189.
22. Forte, E., Barone, M. C., Brunori, M., Sarti, P., and Giuffrè, A. (2002) Redox-linked protonation of cytochrome *c* oxidase: the effect of chloride bound to Cu$_B$. *Biochemistry 43*, 13046−13052.
23. Capitanio, N., Capitanio, G., De Nitto, E., Boffoli, D., and Papa, S. (2003) Proton transfer reactions associated with the reaction of the fully reduced, purified cytochrome *c* oxidase with molecular oxygen and ferricyanide. *Biochemistry 42*, 4607−4612.
24. Wikström, M., Jasaitis, A., Backgren, C., Puustinen, A., and Verkhovsky, M. I. (2000) The role of the D- and K-pathways of proton transfer in the function of the haem-copper oxidases. *Biochim. Biophys. Acta 1459*, 514−520.
25. Ruitenberg, M., Kannt, A., Bamberg, E., Fendler, K., and Michel, H. (2002) Reduction of cytochrome *c* oxidase by a second electron leads to proton translocation. *Nature 417*, 99−102.
26. Ruitenberg, M., Kannt, A., Bamberg, E., Ludwig, B., Michel, H., and Fendler, K. (2000) Single-electron reduction of the oxidized state is coupled to proton uptake via the K pathway in *Paracoccus denitrificans* cytochrome *c* oxidase. *Proc. Natl. Acad. Sci. U.S.A. 97*, 4632−4636.

27. Verkhovsky, M. I., Tuukkanen, A., Backgren, C., Puustinen, A., and Wikström, M. (2001) Charge translocation coupled to electron injection into oxidized cytochrome *c* oxidase from *Paracoccus denitrificans*. *Biochemistry 40*, 7077−7083

28. Hendler, R. W., Pardhasaradhi, K., Reynafarje, B., and Ludwig, B. (1991) Comparison of energy-transducing capabilities of the two- and three-subunit cytochromes *aa₃* from *Paracoccus denitrificans* and the 13-subunit beef heart enzyme. *Biophys. J. 60*, 415−423.

29. Sarti, P., Jones, M. G., Antonini, G., Malatesta, F., Colosimo, A., Wilson, M. T., and Brunori, M. (1985) Kinetics of redox-linked proton pumping activity of native and subunit III-depleted cytochrome *c* oxidase: a stopped-flow investigation. *Proc. Natl. Acad. Sci. U.S.A. 82*, 4876−4880.

30. Scott, R. A., and Gray, H. B. (1980) Cytochrome *aa₃* electron-transfer reactions. Kinetics of hexaammineruthenium (II) reduction of the beef heart enzyme. *J. Am. Chem. Soc. 102*, 3219−3224.

31. Hosler, J. P., Shapleigh, J. P., Mitchell, D. M., Kim, Y., Pressler, M. A., Georgiou, C., Babcock, G. T., Alben, J. O., Ferguson-Miller, S., and Gennis, R. B. (1996) Polar residues in helix VIII of subunit I of cytochrome *c* oxidase influence the activity and the structure of the active site. *Biochemistry 35*, 10776−10783.

32. Vygodina, T. V., Pecoraro, C., Mitchell, D., Gennis, R. B., and Konstantinov, R. B. (1998) Mechanism of inhibition of electron transfer by amino acid replacement K362M in a proton channel of *Rhodobacter sphaeroides* cytochrome *c* oxidase. *Biochemistry 37*, 3053−3061.

33. Giuffrè, A., Barone, M. C., Brunori, M., D'Itri, E., Ludwig, B., Malatesta, F., Mueller, H., and Sarti, P. (2002) Nitric oxide reacts with the single-electron reduced active site of cytochrome *c* oxidase. *J. Biol. Chem. 277*, 22402−22406.

34. Kannt, A., Lancaster, R. D., and Michel, H. (1998) The coupling of electron transfer and proton translocation: electrostatic calculations on *Paracoccus denitrificans* cytochrome *c* oxidase. *Biophys. J. 74*, 708−721.

35. Yoshikawa, S., Shinzawa-Itoh, K., Nakashima, R., Yaono, R., Yamashita, E., Inoue, N., Yao, M., Fei, M. J., Libeu, C. P., Mizushima, T., Yamaguchi, H., Tomizaki, T., and Tsukihara, T. (1998) Redox-coupled crystal structural changes in bovine heart cytochrome *c* oxidase. *Science 280*, 1723−1729.

36. Okuno, D., Iwase, T., Shinzawa-Itoh, K., Yoshikawa, S., and Kitagawa, T. (2003) FTIR detection of protonation/deprotonation of key carboxyl side chains caused by redox change of the Cu(A)-heme *a* moiety and ligand dissociation from the heme *a₃*−Cu(B) center of bovine heart cytochrome *c* oxidase. *J. Am. Chem. Soc. 125*, 7209−7218.

37. Jünemann, S., Meunier, B., Gennis, R. B., and Rich, P. R. (1997) Effects of mutation of the conserved lysine-362 in cytochrome *c* oxidase from *Rhodobacter sphaeroides*. *Biochemistry 36*, 14456−14464.

38. Brändén, M., Tomson, F., Gennis, R. B., and Brzezinski, P. (2002) The entry point of the K-proton-transfer pathway in cytochrome *c* oxidase. *Biochemistry 41*, 10794−10798.

39. Tomson, F., Morgan, J. E., Gu, G., Barquera, B., Vygodina, T. V., and Gennis, R. B. (2003) Substitutions for glutamate 101 in subunit II of cytochrome *c* oxidase from *Rhodobacter sphaeroides* result in blocking the proton-conducting K-channel. *Biochemistry 42*, 1711−1717.

40. Artzatbanov, V. Y., Konstantinov, A. A., and Skulachev, V. P. (1978) Involvement of intramitochondrial protons in redox reactions of cytochrome *a*. *FEBS Lett. 87*, 180−185.